ASME 2012 5th Annual Dynamic Systems and Control Conference joint with the
JSME 2012 11th Motion and Vibration Conference
DSCC2012-MOVIC2012
October 17-19, 2012, Fort Lauderdale, Florida, USA

DSCC2012-MOVIC2012-8752

ADAPTIVE DECENTRALIZED NOISE AND VIBRATION CONTROL WITH CONFLICTING PERFORMANCE OBJECTIVES

E. Dogan Sumer
Department of Aerospace Engineering
University of Michigan
Ann Arbor, Michigan 48109-2140
Email: dogan@umich.edu

Dennis S. Bernstein
Department of Aerospace Engineering
University of Michigan
Ann Arbor, Michigan 48109-2140
Email: dsbaero@umich.edu

ABSTRACT

Decentralized control is a longstanding challenge in systems theory. A decentralized controller may consist of multiple local controllers, connected to disjoint or overlapping sets of sensors and actuators, and where each local controller has limited ability to communicate directly with the remaining local controllers and, in addition, may lack global knowledge of the plant and operation of the remaining local controllers. In the present paper we apply adaptive control to investigate the ability of the local controllers to cooperate globally despite uncertainty, communication constraints, and possibly conflicting performance objectives. The approach we apply in this paper is based on retrospective cost adaptive control (RCAC). The development of RCAC assumes a centralized controller structure; the goal of the present paper is to investigate the stability and performance of RCAC in a decentralized setting.

1 INTRODUCTION

In most applications of control, a single processing unit is used to update the control input; this is the case of centralized control. In many applications, however, the plant is spatially distributed, possibly in the form of a network, and communication constraints make it impractical to update all control inputs using a centralized controller. For example, the electrical power grid involves multiple sectors, which are controlled independently; the challenge is to ensure that overall decentralized control of this system is reliable. Decentralized control is a longstanding challenge in systems theory [1–4].

A decentralized controller may consist of multiple local controllers, connected to disjoint or overlapping sets of sensors and actuators, and where each local controller has limited ability to communicate directly with the remaining local controllers and, in addition, may lack global knowledge of the plant and operation of the remaining local controllers. The local performance objectives of the local controllers are typically consistent in terms of a single global performance objective, although it may be the case that the local performance objectives may conflict, and the challenge is to ensure that the local controllers cooperate so that a measure of global performance is not unnecessarily degraded.

The Witsenhausen counterexample [5, 6] illustrates the difficulties that arise in ensuring global performance objectives based on local information. In particular, communication constraints on the controller structure induce a nonconvex optimization problem that may be computationally intractable.

In the present paper we apply adaptive control to investigate the ability of the local controllers to cooperate globally despite uncertainty, communication constraints, and possibly conflicting performance objectives. This investigation consists of simulations under various decentralized controller architectures to experimentally assess the interplay between local decisions and global performance. The application for this study is active noise control, where it is desirable to implement an active noise control system with independent local controllers that lack the ability to communicate with the other local controllers.

The approach we apply in this paper is based on retrospective cost adaptive control (RCAC). RCAC has the ability to control MIMO systems that are possibly unstable and nonminimum phase under limited modeling information [7–10]. The development of RCAC in [7, 8, 11–13] assumes a centralized controller structure; the goal of this paper is to investigate the stability and performance of RCAC in a decentralized setting. Adaptive techniques for decentralized control are considered in [14–16].

2 Disturbance Rejection Problem

Consider the MIMO discrete-time system

$$x(k+1) = Ax(k) + Bu(k) + D_1 w(k), \tag{1}$$
$$y(k) = Cx(k), \tag{2}$$
$$z(k) = E_1 x(k), \tag{3}$$

where $k \geq 0$, $x(k) \in \mathbb{R}^n$ is the state variable, $z(k) \in \mathbb{R}^{l_z}$ is the measured performance variable to be minimized, $y(k) \in \mathbb{R}^{l_y}$ contains additional measurements that are available for control, $u(k) \in \mathbb{R}^{l_u}$ is the input signal, and $w(k) \in \mathbb{R}^{l_w}$ is the external disturbance signal to be rejected. The system (1)–(3) can represent a sampled-data application arising from a continuous-time system with sample and hold operations with the sampling period h, where $y(k)$ represents $y(kh)$, $z(k)$ represents $z(kh)$, and so on. The plant (1)–(3) is represented by the transfer matrices $G_{yu}(z) \triangleq C(zI-A)^{-1}B$, $G_{yw}(z) \triangleq C(zI-A)^{-1}D_1$, $G_{zu}(z) \triangleq E_1(zI-A)^{-1}B$ and $G_{zw}(z) \triangleq E_1(zI-A)^{-1}D_1$. Furthermore, for a positive integer i, $H_i \triangleq E_1 A^{i-1} B$ is the i^{th} Markov parameter of G_{zu}.

Now, consider the n_{c}^{th}-order strictly proper output feedback controller

$$x_{\text{c}}(k+1) = A_{\text{c}} x_{\text{c}}(k) + B_{\text{c}} y(k), \tag{4}$$
$$u(k) = C_{\text{c}} x_{\text{c}}(k), \tag{5}$$

where $x_{\text{c}}(k) \in \mathbb{R}^{n_{\text{c}}}$. The feedback control (4)–(5) is described by $u(k) = G_{\text{c}}(\mathbf{q})y(k)$, where

$$G_{\text{c}}(\mathbf{q}) = C_{\text{c}}(\mathbf{q}I - A_{\text{c}})^{-1} B_{\text{c}},$$

and $\mathbf{q}$ is the forward shift operator. The closed-loop system with output feedback (4), (5) is thus given by

$$\tilde{x}(k+1) = \tilde{A}\tilde{x}(k) + \tilde{D}_1 w(k), \tag{6}$$
$$y(k) = \tilde{C}\tilde{x}(k), \tag{7}$$
$$z(k) = \tilde{E}_1 \tilde{x}(k), \tag{8}$$

where $\tilde{x} \triangleq \begin{bmatrix} x^{\text{T}} & x_c^{\text{T}} \end{bmatrix}^{\text{T}}$,

$$\tilde{A} = \begin{bmatrix} A & BC_{\text{c}} \\ B_{\text{c}}C & A_{\text{c}} \end{bmatrix}, \quad \tilde{D}_1 = \begin{bmatrix} D_1 \\ 0_{n_{\text{c}} \times l_w} \end{bmatrix}, \tag{9}$$
$$\tilde{C} = \begin{bmatrix} C & 0_{l_y \times n_{\text{c}}} \end{bmatrix}, \quad \tilde{E}_1 = \begin{bmatrix} E_1 & 0_{l_z \times n_{\text{c}}} \end{bmatrix}. \tag{10}$$

The closed-loop system (6)–(8) is described by

$$\begin{bmatrix} z \\ y \end{bmatrix}^{\text{T}} = \tilde{G}(z)w = \begin{bmatrix} \tilde{G}_{zw}(z) \\ \tilde{G}_{yw}(z) \end{bmatrix}^{\text{T}} w,$$

where

$$\tilde{G}_{yw}(z) = \tilde{C}(zI - \tilde{A})^{-1}\tilde{D}_1, \tag{11}$$
$$\tilde{G}_{zw}(z) = \tilde{E}_1(zI - \tilde{A})^{-1}\tilde{D}_1. \tag{12}$$

The goal of the adaptive disturbance rejection problem is to develop an adaptive output feedback controller of the form (4), (5) that minimizes the performance measure $z^{\text{T}}z$ in the presence of the exogenous signal w with limited modeling information about the dynamics and the exogenous signal. For the adaptive system, the matrices in (4), (5) may be time varying, and thus the transfer function models (11), (12) may not be valid during controller adaptation. However, (11), (12) illustrates the structure of the closed-loop system after controller convergence.

Decentralized adaptive control problem is an extension of the adaptive disturbance rejection problem, where the goal is to have multiple adaptive controllers $G_{\text{c},i}$ which generate a control signal $u_i(k)$ using a measurement $y_i(k)$. The objective of each controller is to minimize a performance measure $z_i^{\text{T}} z_i$ in the presence of the exogenous signal w as well as the control signals generated by the remaining decentralized controllers which may have conflicting performance objectives. Decentralized adaptive architecture is shown in Figure 1 for two controllers.

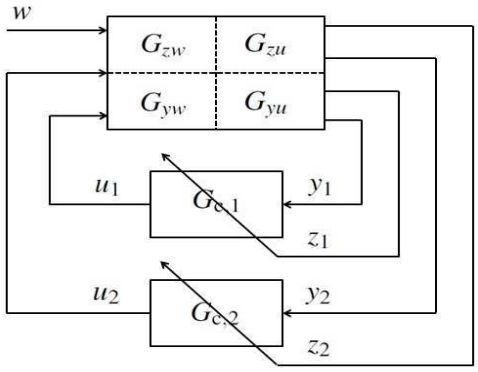

Figure 1. DECENTRALIZED ADAPTIVE CONTROL ARCHITECTURE WITH TWO CONTROLLERS.

3 RETROSPECTIVE COST ADAPTIVE CONTROL

3.1 Control Law

We represent Eqs. (4), (5) by

$$u(k) = \theta^{\text{T}}(k)\phi(k-1), \tag{13}$$

where

$$\theta(k) = \left[N_1^{\mathrm{T}}(k) \ \cdots \ N_{n_c}^{\mathrm{T}}(k) \ M_1^{\mathrm{T}}(k) \ \cdots \ M_{n_c}^{\mathrm{T}}(k)\right]^{\mathrm{T}}, \tag{14}$$

$$\phi(k-1) = \left[y^{\mathrm{T}}(k-1) \ \cdots \ y^{\mathrm{T}}(k-n_c) \ u^{\mathrm{T}}(k-1) \ \cdots \ u^{\mathrm{T}}(k-n_c)\right]^{\mathrm{T}}, \tag{15}$$

and, for all $1 \le i \le n_c$, $N_i(k) \in \mathbb{R}^{l_y \times l_u}$, $M_i(k) \in \mathbb{R}^{l_u \times l_u}$. The control law (13) can be reformulated as

$$u(k) = \Phi(k-1)\Theta(k), \tag{16}$$

where

$$\Phi(k-1) \triangleq I_{l_u} \otimes \phi^{\mathrm{T}}(k-1) \in \mathbb{R}^{l_u \times l_u n_c (l_u+l_y)}, \tag{17}$$

$$\Theta(k) \triangleq \mathrm{vec}(\theta(k)) \in \mathbb{R}^{l_u n_c (l_u+l_y)}, \tag{18}$$

"$\otimes$" denotes the Kronecker product, and "vec" is the column-stacking operator.

3.2 Retrospective Performance

For a positive integer n_f, we define

$$G_f(\mathbf{q}) \triangleq D_f^{-1}(\mathbf{q}) N_f(\mathbf{q}) \in \mathbb{R}^{l_z \times l_u}[\mathbf{q}], \tag{19}$$

where

$$\begin{aligned} N_f(\mathbf{q}) &\triangleq K_1 \mathbf{q}^{n_f-1} + K_2 \mathbf{q}^{n_f-2} + \cdots + K_{n_f}, \\ D_f(\mathbf{q}) &\triangleq I_{l_z} \mathbf{q}^{n_f} + A_1 \mathbf{q}^{n_f-1} + A_2 \mathbf{q}^{n_f-2} + \cdots + A_{n_f}, \end{aligned} \tag{20}$$

$K_i \in \mathbb{R}^{l_z \times l_u}$ for $1 \le i \le r$, $A_j \in \mathbb{R}^{l_z \times l_z}$ for $1 \le j \le r$, $n_f \ge 1$ is the order of G_f, and each polynomial entry of $D_f(\mathbf{q})$ is asymptotically stable. Next, for $k \ge 1$, we define the *retrospective performance variable*

$$\hat{z}(\hat{\Theta}(k), k) \triangleq z(k) + \Phi_f(k-1)\hat{\Theta}(k) - u_f(k), \tag{21}$$

with

$$\Phi_f(k-1) \triangleq G_f(\mathbf{q})\Phi(k-1) \in \mathbb{R}^{l_z \times l_u n_c (l_u+l_y)}, \tag{22}$$

$$u_f(k) \triangleq G_f(\mathbf{q})u(k) \in \mathbb{R}^{l_z}, \tag{23}$$

where $\hat{\Theta}(k)$ is determined by optimization below.

In this paper, we choose G_f as a finite-impulse-response filter so that $A_i = 0$ for all $i \in \{1, \ldots, n_f\}$. The choice of G_f is further discussed in Section 4.

3.3 Cumulative Cost and Update Law

For $k > 0$, we define the cumulative cost function

$$\begin{aligned} J(\hat{\Theta}(k), k) \triangleq & \sum_{i=1}^{k} \lambda^{k-i} \hat{z}^{\mathrm{T}}(\hat{\Theta}(k), i)\hat{z}(\hat{\Theta}(k), i) \\ & + \sum_{i=1}^{k} \lambda^{k-i} \eta(i) \hat{\Theta}^{\mathrm{T}}(k) \Phi_f^{\mathrm{T}}(i-1)\Phi_f(i-1)\hat{\Theta}(k) \\ & + \lambda^k (\hat{\Theta}(k) - \Theta_0)^{\mathrm{T}} P_0^{-1} (\hat{\Theta}(k) - \Theta_0), \end{aligned} \tag{24}$$

where $\lambda \in (0, 1]$, $P_0 \in \mathbb{R}^{l_u n_c (l_u+l_y) \times l_u n_c (l_u+l_y)}$ is positive definite, $\eta(k) \ge 0$, and $\Theta_0 \in \mathbb{R}^{l_u n_c (l_u+l_y)}$. In this paper, we choose

$$\eta(k) \triangleq \eta_0 \sum_{j=0}^{p_c-1} z^{\mathrm{T}}(k-j) z(k-j). \tag{25}$$

where $\eta_0 \ge 0$, and $p_c \ge 1$. The following result provides the global minimizer of the cost function (24).

Proposition 3.1. Let $P(0) = P_0$ and $\Theta(0) = \Theta_0$. Then, for all $k \ge 1$, the cumulative cost function (24) has a unique global minimizer $\Theta(k)$. Furthermore, $\Theta(k)$ is given by

$$\Theta(k) = \Theta(k-1) - \frac{1}{1+\eta(k)} P(k-1)\Phi_f^{\mathrm{T}}(k-1)\Lambda^{-1}(k)\varepsilon(k), \tag{26}$$

where

$$\begin{aligned} \Lambda(k) &\triangleq \frac{\lambda}{1+\eta(k)} I_{l_z} + \Phi_f(k-1)P(k-1)\Phi_f^{\mathrm{T}}(k-1), \\ \varepsilon(k) &\triangleq z(k) - u_f(k) + (1+\eta(k))\hat{u}_f(k), \\ \hat{u}_f(k) &\triangleq \Phi_f(k-1)\Theta(k-1), \end{aligned}$$

and $P(k)$ satisfies

$$\begin{aligned} P(k) = \frac{1}{\lambda}[&P(k-1) \\ &- P(k-1)\Phi_f^{\mathrm{T}}(k-1)\Lambda^{-1}(k)\Phi_f(k-1)P(k-1)]. \end{aligned} \tag{27}$$

Proof 3.1. The result follows from RLS theory [17, 18].

4 CONSTRUCTION OF G_{f} BASED ON PHASE MATCHING

The phase-matching-based construction of G_{f} is applicable to plants that are either minimum-phase or Lyapunov stable, and does not require knowledge of the NMP zeros of the plant. For NMP systems, this construction requires that η_0 be positive. For unstable, NMP plants, knowledge of the NMP zero locations may be necessary [8, 12].

Let $G_{z_i u_j}$ denote the transfer function from the j^{th} input $u_j \in \mathbb{R}$ to the i^{th} performance output $z_i \in \mathbb{R}$. Furthermore, let $G_{\mathrm{f},ij}$ denote the ij^{th} entry of G_{f}. Then, for $\Omega \in [0,\pi]$ rad/sample, the *phase mismatch* $\Delta_{ij}(\Omega)$ between $G_{\mathrm{f},ij}$ and $G_{z_i u_j}$ is defined as

$$\Delta_{ij}(\Omega) \triangleq \cos^{-1} \frac{\mathrm{Re}\left[G_{z_i u_j}(e^{\mathrm{j}\Omega})\overline{G_{\mathrm{f},ij}(e^{\mathrm{j}\Omega})}\right]}{\left|G_{z_i u_j}(e^{\mathrm{j}\Omega})\right|\left|G_{\mathrm{f},ij}(e^{\mathrm{j}\Omega})\right|} \in [0,180]. \quad (28)$$

For the phase-matching-based construction, we construct G_{f} such that, for each input-output pair ij, $1 \le i \le l_z$, $1 \le j \le l_u$, the channel-wise phase mismatch is smaller than 90 deg, that is,

$$\Delta_{ij}(\Omega) \le 90 \text{ deg}, \text{for all } \Omega \in [0,\ \pi] \text{ rad/sample}, \quad (29)$$

A weaker condition is sufficient when G_{zu} is asymptotically stable, and the exogenous signal $w(k)$ is harmonic. In this case, the phase-mismatch-based construction requires

$$\Delta(\Omega_i) \le 90 \text{ deg}, \Omega \in \text{spec}(w), \quad (30)$$

where "spec(w)" is the frequency spectrum of w.

Two methods for minimizing phase mismatch are presented in [19]. These methods fit the IIR plant $G_{z_i u_i}$ with an FIR transfer function $G_{\mathrm{f},ij}$ to bound or minimize the phase mismatch. In particular, one method solves a constrained linear least squares problem to bound $\Delta_{ij}(\Omega)$, while the other method solves a nonlinear least squares problem to minimize $\Delta_{ij}(\Omega)$. The former requires an estimate of the frequency response $G_{z_i u_i}(e^{\mathrm{j}\Omega})$ for $\Omega \in [0,\ \pi]$ (or for $\Omega \in \text{spec}(w)$), while the latter requires an estimate of the phase $\angle G_{z_i u_i}(e^{\mathrm{j}\Omega})$ for $\Omega \in [0,\ \pi]$ (or for $\Omega \in \text{spec}(w)$.) Although these methods parameterize the fit with an FIR plant, greater flexibility may be obtained by allowing G_{f} to be a stable IIR filter. When the nonlinear fitting method is used, only the phase difference is minimized, therefore, the magnitude of the FIR fit may be arbitrary. In this case, considering the robustness margins presented in [11], we typically normalize the leading coefficient of G_{f} to H_1.

5 SIMULATION RESULTS

5.1 Decentralized Disturbance Rejection on an Acoustic Duct

Consider the acoustic duct shown in Fig. 2 with five equally spaced speakers and microphones. The equations of motion for the duct are given by [20]

$$\frac{1}{c^2} p_{tt}(\xi,t) = p_{\xi\xi}(\xi,t) + \sum_{i=1}^{5} \rho_0 \dot{v}_{\mathrm{v}_i}(t)\delta(\xi-\xi_i),$$
$$\zeta_i(t) = p_{\xi_i,t},$$

where $p(\xi,t)$ is the acoustic pressure, c is the phase speed of the acoustic wave (343 m/sec in air at room conditions), v_{v_i} are the speaker cone velocities (m/sec), and ρ_0 is the equilibrium density of air (1.21 kg/m^3 at room conditions). By using separation of variables, retaining r modal frequencies, $p(\xi,t)$ is given by

$$p(\xi,t) = \sum_{i=0}^{r} q_i(t) V_i(\xi).$$

The state space realization of the system is given by

$$\dot{\chi}(t) = \bar{A}\chi(t) + \bar{B}\mathrm{v}(t)$$
$$\zeta(t) = \bar{E}_1\chi(t)$$

where

$$\chi(t) \triangleq \left[\ \textstyle\int_0^t q_1(\tau)\mathrm{d}\tau \ \ q_1(t) \ \ \cdots \ \ \int_0^t q_r(\tau)\mathrm{d}\tau \ \ q_r(t)\ \right]^{\mathrm{T}},$$
$$\mathrm{v}(t) \triangleq \left[\ \mathrm{v}_1(t) \ \cdots \ \mathrm{v}_5(t)\ \right]^{\mathrm{T}} = A_{\mathrm{s}}\left[\ v_{\mathrm{v}_1}(t) \ \cdots \ v_{\mathrm{v}_5}(t)\ \right]^{\mathrm{T}},$$
$$\zeta(t) \triangleq \left[\ \zeta_1(t) \ \cdots \ \zeta_5(t)\ \right]$$
$$\bar{A} \triangleq \begin{bmatrix} 0 & 1 & 0 & \cdots & 0 \\ -\omega_{\mathrm{n}1}^2 & -2\mu_1\omega_{\mathrm{n}1} & 0 & \cdots & 0 \\ 0 & 0 & \ddots & & \\ \vdots & \vdots & & 0 & 1 \\ 0 & 0 & \cdots & -\omega_{\mathrm{n}r}^2 & -2\mu_r\omega_{\mathrm{n}r} \end{bmatrix}$$
$$\bar{B} \triangleq \left[\ \bar{b}_1 \cdots \bar{b}_5\ \right],\ \bar{b}_i \triangleq \left[\ 0\ \tfrac{\rho_0}{A_{\mathrm{s}}} V_1(\xi_i) \ \cdots \ 0\ \tfrac{\rho_0}{A_{\mathrm{s}}} V_r(\xi_i)\ \right]^{\mathrm{T}}$$
$$\bar{E}_1 \triangleq \begin{bmatrix} \bar{e}_1 \\ \vdots \\ \bar{e}_5 \end{bmatrix}, \qquad \bar{e}_i \triangleq \left[\ 0\ V_1(\xi_i) \ \cdots \ 0\ V_r(\xi_i)\ \right]$$

and

$$\omega_{\mathrm{n}i} \triangleq \frac{i\pi}{L}c, \quad V_i(\xi) \triangleq c\sqrt{\frac{2}{L}}\sin(\frac{i\pi}{L}\xi), \quad i = 1,\ 2,\ \cdots,\ r$$

where A_s is the cross-sectional area of the speaker, μ_i is the damping ratio of the i^{th} acoustic mode, and L is the length of the duct. In the examples of this section, we let $A_s = 0.0025$ m^2, $L = 3$ m, $\mu_j = 0.1$, $j = 1,\cdots,4$, and $\xi_i = 0.3 + (i-1)0.6$ m, $i = 1,\cdots,5$. In each example, we sample the continuous-time system with the sampling period $h = 0.005$ sec/sample using zero-order hold. The sampling rate is chosen to be large enough to capture the fast modes of the system. In all examples, we assume that the performance measurement z_i is the input to the i^{th} decentralized controller $G_{c,i}$, that is, $y_i = z_i$ for all controllers. Finally, in each case, we assume that the phase plot and the first Markov parameter of $G_{z_iu_i}$ is available for each decentralized controller.

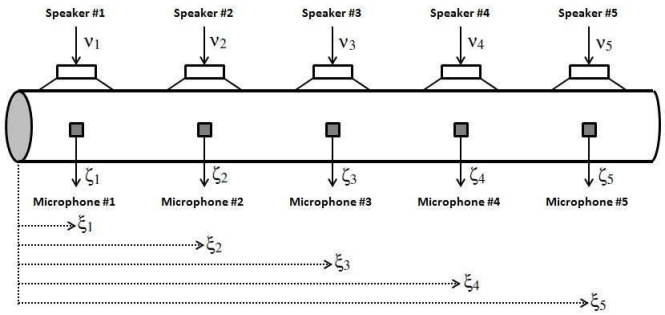

Figure 2. ACOUSTIC DUCT.

Example 5.1. [Decentralized Disturbance Rejection with Shared Performance Measure.] Consider two RCAC controllers $G_{c,1}$, $G_{c,2}$ connected to the acoustic duct as in Figure 1. The controllers are placed symmetrically so that $G_{c,1}$ actuates on speaker $S2$, that is, $u_1(k) = \nu_2(kh)$, $G_{c,2}$ actuates on speaker $S4$, that is, $u_2(k) = \nu_4(kh)$, and the performance objective for both controllers is to minimize the acoustic pressure $\zeta_3(kh)$, therefore, $z_1(k) = z_2(k) = \zeta_3(kh)$, in the presence of the disturbance $w(k) = \nu_3(kh)$ generated by speaker $S3$. Because of the symmetry between the controllers, the sampled-data transfer functions $G_{z_1u_1}(z)$ and $G_{z_2u_2}(z)$ are equal, whose pole-zero configurations are shown in Figure 3. Furthermore, $H_1 = 9706.9$ for both transfer functions. Using the phase information, we apply the nonlinear fitting method [19] to minimize the phase mismatch and obtain

$$G_{f,1}(\mathbf{q}) = G_{f,2}(\mathbf{q}) = K_f \begin{bmatrix} \mathbf{q}^{-1} & \cdots & \mathbf{q}^{-15} \end{bmatrix}^{\mathrm{T}}, \tag{31}$$

where

$$K_f = \kappa \big[1 \;\; 0.94 \;\; 0.93 \;\; 0.83 \;\; 0.65 \;\; 0.38 \;\; 0.04 \;\; -0.3 \;\; -0.6 \;\; -0.79 \;\; -0.87 \;\; -0.82 \;\; -0.68 \;\; -0.48 \;\; -0.24 \big] \tag{32}$$

and $\kappa > 0$. Note that the choice of κ does not affect the phase of G_f and thus the phase mismatch, and, as stated in Section 4, κ is typically normalized to H_1 when one centralized controller is constructed with nonlinear fitting method. However, for reasons explained below, we choose $\kappa = 2H_1$.

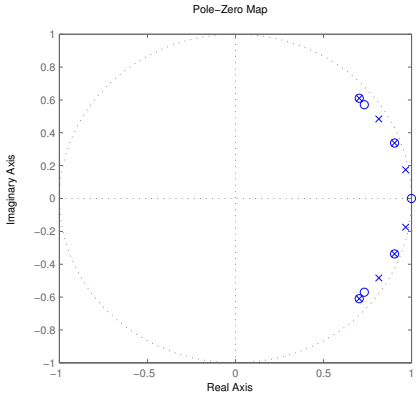

Figure 3. POLES AND ZEROS OF $G_{z_1u_1}(z)$ AND $G_{z_2u_2}(z)$.

We consider the sinusoidal disturbance $\nu_3(t) = 10^{-5}(\sin\omega_1 t + \mathbf{1}(t-1)\sin\omega_2 t)$ m^3/sec, where $\omega_1 = 1.257$ kHz and $\omega_2 = 0.838$ kHz. Furthermore, we assume that at $t = 0.5$ sec, speaker $S2$ experiences damage and loses the ability to actuate.

Both controllers are chosen to be of order $n_c = 15$, and the RLS covariance matrix for each controller is initialized from $P_0 = I$. The plant is allowed to operate in open-loop for 100 time steps, and at $k = 100$ (that is, $t = 0.1$), both controllers are turned on. The acoustic pressure $\zeta_3(kh)$, which is the performance measurement, is driven to zero, $G_{c,2}$ readapts to counter the speaker damage at $k = 1000$, and it further adapts when the second sinusoidal component of $w(k)$ appears at $k = 2000$, as shown in Figure 4.

In (32), contrary to the description in Section 4, we chose the leading coefficient κ to be equal to $2H_1$, instead of H_1. Poor results are obtained with $\kappa = H_1$, and, if κ is further reduced below H_1, instability is observed. This is because the total control input $u(k) = u_1(k) + u_2(k)$ generated by the two symmetrically placed, uncoordinated controllers is twice as large as the required control level. Therefore, to reduce the control effort generated by each decentralized controller, we multiply $G_{f,1}$ and $G_{f,2}$ by $2H_1$, that is, twice the constant that is used with a centralized controller. ■

Example 5.2. [Decentralized Disturbance Rejection with Separate Performance Measures.] Consider two RCAC controllers $G_{c,1}$, $G_{c,2}$ connected to the acoustic duct as in Figure 1. The controllers are placed on both edges of the duct so that $G_{c,1}$ actuates speaker $S1$, that is, $u_1(k) = \nu_1(kh)$, $G_{c,2}$ actuates speaker $S5$, that is, $u_2(k) = \nu_5(kh)$. The controllers now have separate performance objectives; $z_1(k) = \zeta_1(kh)$, whereas $z_2(k) = \zeta_5(kh)$, and the disturbance signal $w(k)$ is generated by speaker $S2$. Because of the symmetry between the controllers and the performance measurements, the sampled-data transfer functions $G_{z_1u_1}(z)$ and $G_{z_2u_2}(z)$ are equal, whose pole-zero configurations are shown in Figure 5. Furthermore, $H_1 = 33831$ for

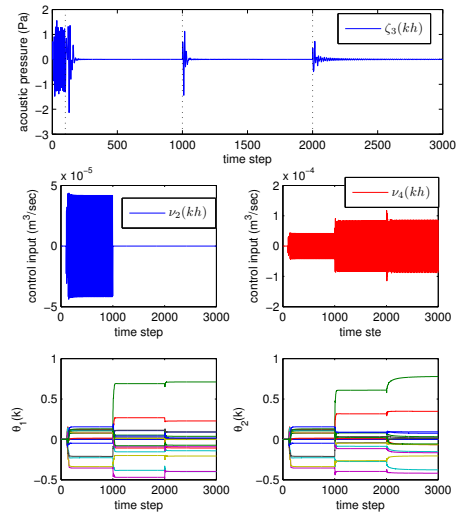

Figure 4. SIMULATION RESULTS FOR EX. 5.1: TWO DECENTRALIZED RCAC CONTROLLERS ARE TURNED ON AT $k = 100$ TO MINIMIZE THE SHARED PERFORMANCE MEASURE $z(k) = \zeta_3(kh)$. AT $k = 1000$, SPEAKER $S2$ EXPERIENCES DAMAGE AND $G_{c,1}$ LOSES THE ABILITY TO ACTUATE. $G_{c,2}$ READAPTS TO COUNTER THE SPEAKER FAILURE AND THE ADDITIONAL COMPONENT OF THE DISTURBANCE THAT APPEARS AT $k = 2000$.

both transfer functions. Using the phase information, we apply the nonlinear fitting method [19] to minimize the phase mismatch and obtain

$$G_{f,1}(\mathbf{q}) = G_{f,2}(\mathbf{q}) = \kappa \frac{\mathbf{q}^4 + 0.3771\mathbf{q}^3 - 0.2711\mathbf{q}^2 - 0.6127\mathbf{q} - 0.4933}{\mathbf{q}^5},$$

where κ is chosen to be H_1, since the performance measures are separate.

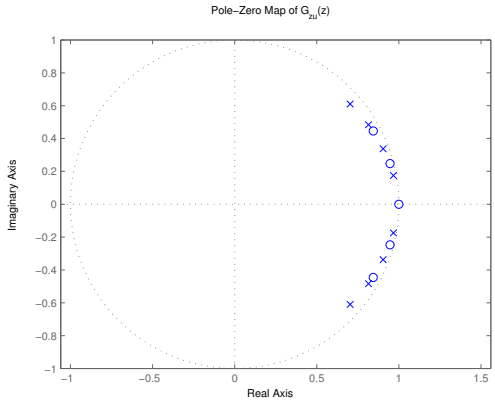

Figure 5. POLES AND ZEROS OF $G_{z_1u_1}(z)$ AND $G_{z_2u_2}(z)$.

We consider the sinusoidal disturbance $\nu_2(t) = 10^{-3}\sin\omega t$ $\mathrm{m}^3/\mathrm{sec}$, where $\omega = 2.513$ kHz, hence, $w(k) = 10^{-3}\sin\Omega k$, $\Omega =$ 1.2566 rad/sample. The controllers interact with the duct as follows. First, for 500 time steps, the duct is allowed to run open-loop. Next, at $k = 500$, $G_{c,1}$ is turned on for minimizing the acoustic pressure $\zeta_1(kh)$. At $k = 1500$, the parameters θ_1 of $G_{c,1}$ are frozen, and $G_{c,2}$ is turned on for minimizing the acoustic pressure $\zeta_5(kh)$. Finally, at $k = 2500$, $G_{c,1}$ is allowed to adapt again, and both controllers adapt simultaneously. The tuning parameters are chosen to be $n_{c,1} = 4$, $n_{c,2} = 2$, $P_{0,1} = 0.001I$, $P_{0,2} = 0.005I$, $\eta_{0,1} = 0.005$, $p_{c,1} = 10$, $\eta_{0,2} = 0.001$, and $p_{c,2} = 10$. Even though $G_{z_iu_i}$ are minimum-phase for $i = 1,2$, we choose nonzero $\eta_{0,i}$ to bound the control amplitude during the transient period for better transient performance. The closed-loop response is illustrated in Figure 6. The closed-loop suppression levels at $k = 1500, 2500$ and 3000 are compared with the open-loop level in Figure 7. ■

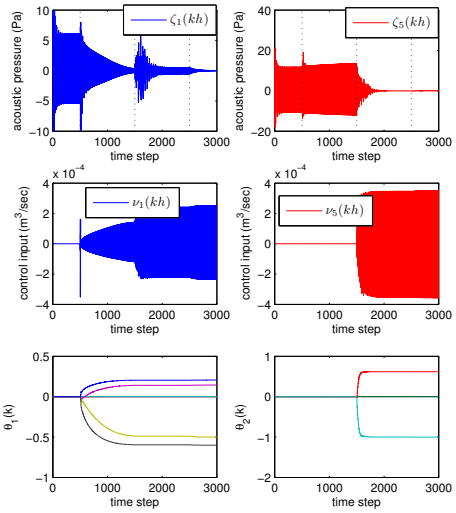

Figure 6. EX. 5.2: TWO DECENTRALIZED RCAC CONTROLLERS ACTUATING SPEAKERS $S1$ AND $S5$ WITH SEPARATE PERFORMANCE OBJECTIVES. AT $k = 500$, $G_{c,1}$ IS ACTIVATED AND DRIVES THE ACOUSTIC PRESSURE $\zeta_1(kh)$ AT MICROPHONE $M1$ TO ZERO. NEXT, AT $k = 1500$, THE PARAMETERS OF $G_{c,1}$ ARE FROZEN, $G_{c,2}$ IS ACTIVATED AND DRIVES $\zeta_5(kh)$ TO ZERO, BUT DISRUPTS $\zeta_1(kh)$. FINALLY, AT $k = 2500$, $G_{c,1}$ IS ALLOWED TO ADAPT AGAIN TO DRIVE $\zeta_1(kh)$ BACK TO ZERO.

5.2 Decentralized Disturbance Rejection for a Lumped-Parameter Structure

Consider the multiple degrees-of-freedom (MDOF) r-mass lumped parameter structure with shown in Fig. 8. The equations of motion for this system are given by

$$M\ddot{q} + C_d\dot{q} + Kq = B_0 f + D_w\bar{w}, \tag{33}$$

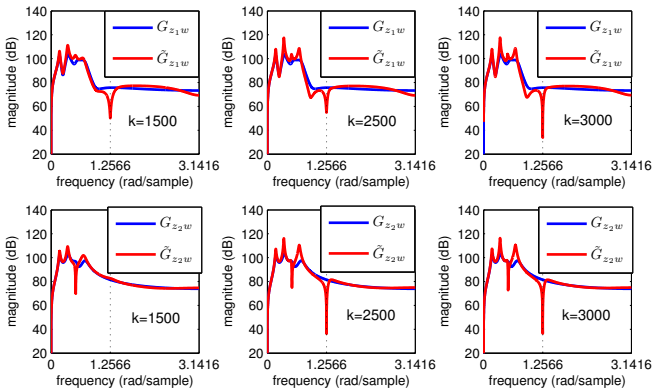

Figure 7. OPEN-LOOP AND CLOSED-LOOP BODE MAGNITUDE PLOTS IN EX. 5.2 AT TIME STEPS $k = 1500, 2500$ AND 3000. BLUE REPRESENTS OPEN-LOOP, RED REPRESENTS CLOSED-LOOP. THE FIRST ROW SHOWS $G_{z_1 w}$, WHEREAS THE SECOND ROW SHOWS $G_{z_2 w}$. COMPARED TO THE OPEN-LOOP LEVELS, ABOUT 45 dB MORE SUPPRESSION IS OBTAINED AT THE COMMAND FREQUENCY 1.2566 RAD/SAMPLE IN BOTH CHANNELS AT $k = 3000$.

where $q = \begin{bmatrix} q_1 & \cdots & q_r \end{bmatrix} \in \mathbb{R}^r$ is the displacement vector, M, $C_{\rm d}$ and K are the mass, damping and stiffness matrices respectively, and are given by $M = \mathrm{diag}(m_1, \ldots, m_r)$,

$$C_{\rm d} = \begin{bmatrix} c_1+c_2 & -c_2 & 0 & \cdots & & 0 \\ -c_2 & c_2+c_3 & -c_3 & 0 & \cdots & 0 \\ & \ddots & \ddots & \ddots & \ddots & \vdots \\ 0 & \cdots & -c_{r-1} & c_{r-1}+c_r & -c_r & 0 \\ 0 & \cdots & & 0 & -c_r & c_r+c_{r+1} \end{bmatrix}$$

$$K = \begin{bmatrix} k_1+k_2 & -k_2 & 0 & \cdots & & 0 \\ -k_2 & k_2+k_3 & -k_3 & 0 & \cdots & 0 \\ & \ddots & \ddots & \ddots & \ddots & \vdots \\ 0 & \cdots & -k_{r-1} & k_{r-1}+k_r & -k_r & 0 \\ 0 & \cdots & & 0 & -k_r & k_r+k_{r+1} \end{bmatrix}.$$

The control input to the system is the force $f \in \mathbb{R}^{l_u}$, and the disturbance signal is given by $\bar{w} \in \mathbb{R}^{l_w}$. The outputs are

$$y(t) = \begin{bmatrix} C_0 & C_1 \end{bmatrix} \begin{bmatrix} q \\ \dot{q} \end{bmatrix}, \tag{34}$$

$$z(t) = \begin{bmatrix} E_{\rm p} & E_{\rm v} \end{bmatrix} \begin{bmatrix} q \\ \dot{q} \end{bmatrix}, \tag{35}$$

where $z(t) \in \mathbb{R}^{l_z}$ is the performance measurement, and $y(t) \in \mathbb{R}^{l_y}$ contains measurements available for feedback. We can write (33)–(35) in state-space form as

$$\dot{\chi}(t) = \bar{A}\chi(t) + \bar{B}\bar{u}(t) + \bar{D}_1\bar{w}(t), \tag{36}$$

$$y(t) = \bar{C}\chi(t), \tag{37}$$

$$z(t) = \bar{E}_1\chi(t), \tag{38}$$

where

$$\bar{A} \triangleq \begin{bmatrix} 0 & I_r \\ -M^{-1}K & -M^{-1}C_{\rm d} \end{bmatrix} \quad \bar{B} \triangleq \begin{bmatrix} 0_{r\times l_u} \\ M^{-1}B_0 \end{bmatrix}, \quad \bar{D}_1 \triangleq \begin{bmatrix} 0_{r\times l_w} \\ M^{-1}D_w \end{bmatrix},$$

$$\bar{C} \triangleq \begin{bmatrix} C_0 & C_1 \end{bmatrix}, \quad \bar{E}_1 \triangleq \begin{bmatrix} E_{\rm p} & E_{\rm v} \end{bmatrix} \quad \chi(t) \triangleq \begin{bmatrix} q(t) & \dot{q}(t) \end{bmatrix}, \; \bar{u}(t) \triangleq f(t).$$

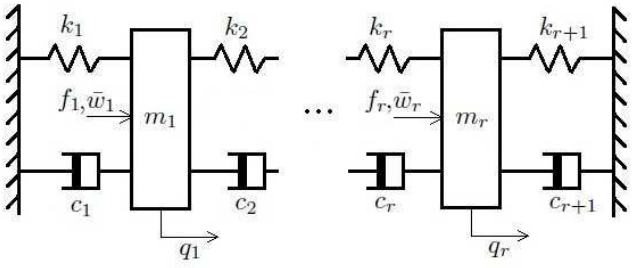

Figure 8. AN r-MASS LUMPED PARAMETER STRUCTURE.

In each example, we sample the continuous-time system (36)–(38) with the sampling period $h = 0.2$ sec/sample using zero-order hold to obtain the sampled-data plant (1)–(3). Each example is constructed so that the sampling rate is sufficiently large to capture the fastest mode of the plant, and the disturbance frequency is chosen smaller than the Nyquist rate to prevent aliasing. Finally, in all examples, we assume that the performance measurement z_i is the input to the $i^{\rm th}$ decentralized controller $G_{{\rm c},i}$, that is, $y_i = z_i$ for all controllers.

Example 5.3. [Decentralized Disturbance Rejection with Separate Performance Measures.] Consider a 3DOF lumped parameter structure with the masses $m_1 = 1.1$ kg, $m_2 = 1.2kg$, $m_3 = 1kg$; spring constants $k_1 = 0.7$ kg/sec^2, $k_2 = 3$ kg/sec^2, $k_3 = 2.3$ kg/sec^2, $k_4 = 1$ kg/sec^2; and the damping coefficients $c_1 = 1.5$ kg/sec, $c_2 = 0.5$ kg/sec, $c_3 = 0.8$ kg/sec, and $c_4 = 1$ kg/sec. With these parameters, every eigenvalue of $\bar{A}$ lies in the open left-half plane, and thus the structure is asymptotically stable.

Consider two RCAC controllers $G_{{\rm c},1}$, $G_{{\rm c},2}$ connected to the structure as in Figure 1. The controller $G_{{\rm c},1}$ applies a force $f_1(kh)$ on m_1, and the controller $G_{{\rm c},2}$ applies a force $f_3(kh)$ on m_3, that is, $u_1(k) = f_1(kh)$, $u_2(k) = f_3(kh)$ (see Figure 8). The controllers have separate performance objectives; $z_1(k) = q_1(kh)$, whereas $z_2(k) = q_3(kh)$, and there is a disturbance force $\bar{w}_2(t)$

exerted on the mass m_2. The goal of each decentralized controller is to reject the disturbance force from the corresponding performance variable. Pole-zero configurations of the sampled-data plants $G_{z_1u_1}(z)$ and $G_{z_2u_2}(z)$ are shown in Figure 9. Both channels have a minimum-phase sampling zero near -0.7. Furthermore, the first Markov parameter corresponding to $G_{z_1u_1}$ is $H_{1,1} = 0.0132$, and the first Markov parameter corresponding to $G_{z_2u_2}$ is $H_{1,2} = 0.0144$. Using the phase information of the sampled-data channels, we apply the nonlinear fitting method [19] to minimize the phase mismatch in both channels, and obtain

$$G_{c,1}(\mathbf{q}) = H_{1,1}(\mathbf{q}^{-1} + 0.9318\mathbf{q}^{-2}),$$
$$G_{c,2}(\mathbf{q}) = H_{1,2}(\mathbf{q}^{-1} + 0.9297\mathbf{q}^{-2}).$$

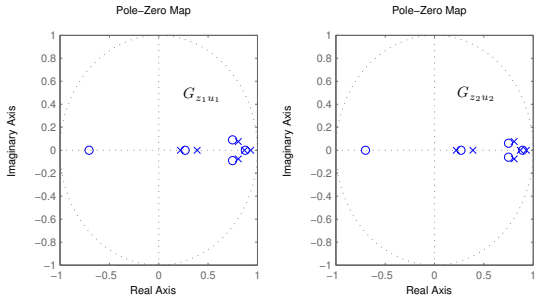

Figure 9. POLES AND ZEROS OF $G_{z_1u_1}(z)$ AND $G_{z_2u_2}(z)$.

We consider the sinusoidal disturbance force $\bar{w}_2(t) = 100\sin\omega t$ N, where $\omega = 5.236$ Hz, hence, $w(k) = 100\sin\Omega k$, $\Omega = 1.0472$ rad/sample. The controllers interact with the structure as follows. First, for 500 time steps, the duct is allowed to run open-loop. Next, at $k = 500$, $G_{c,1}$ is turned on for minimizing the displacement $q_1(kh)$. At $k = 1500$, the parameters θ_1 of $G_{c,1}$ are frozen, and $G_{c,2}$ is turned on for minimizing the displacement $q_3(kh)$. Finally, at $k = 2500$, $G_{c,1}$ is allowed to adapt again, and both controllers adapt simultaneously. The tuning parameters are chosen to be $n_c = 4$, $P_0 = 10^{10}I$, $\eta_0 = 0$ for both controllers. The closed-loop response is illustrated in Figure 10. Unlike Ex. 5.2, the decentralized controllers do not significantly disrupt the performance measure of each other. This is because the bode gains of $G_{z_1u_2}$ and $G_{z_2u_1}$ at the disturbance frequency are significantly lower than the gains of $G_{z_1u_1}$ and $G_{z_2u_2}$. The closed-loop suppression levels at $k = 1500, 2500$ and 3000 are compared with the open-loop level in Figure 11. ■

Example 5.4. [Decentralized Disturbance Rejection in the Presence of Unknown NMP Zeros.] Consider a 4DOF lumped parameter structure with the masses $m_1 = 0.5$ kg, $m_2 = 1.2kg$, $m_3 = 1.4kg$, $m_4 = 0.4$ kg; spring constants $k_1 = 0.5$ kg/sec^2, $k_2 = 3.5$ kg/sec^2, $k_3 = 2$ kg/sec^2, $k_4 = 3$ kg/sec^2, $k_5 = 1$ kg/sec^2; and the damping coefficients $c_1 = 1.7$ kg/sec, $c_2 = 2.6$ kg/sec, $c_3 = 2.3$ kg/sec, $c_4 = 2.5$ kg/sec, and $c_5 = 1.8$ kg/sec. With

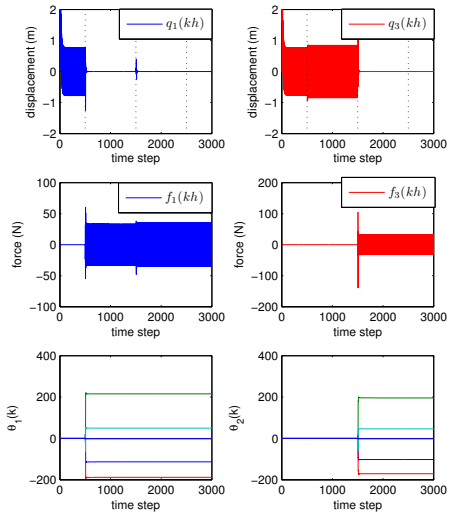

Figure 10. EX. 5.3: TWO DECENTRALIZED RCAC CONTROLLERS EXERTING FORCES f_1 AND f_3 WITH SEPARATE PERFORMANCE OBJECTIVES. AT $k = 500$, $G_{c,1}$ IS ACTIVATED AND DRIVES THE PERFORMANCE DISPLACEMENT $q_1(kh)$ TO ZERO. NEXT, AT $k = 1500$, THE PARAMETERS OF $G_{c,1}$ ARE FROZEN, $G_{c,2}$ IS ACTIVATED AND DRIVES $q_3(kh)$ TO ZERO. THE ACTIVATION OF $G_{c,2}$ DOES NOT SIGNIFICANTLY AFFECT THE DISPLACEMENT q_1.

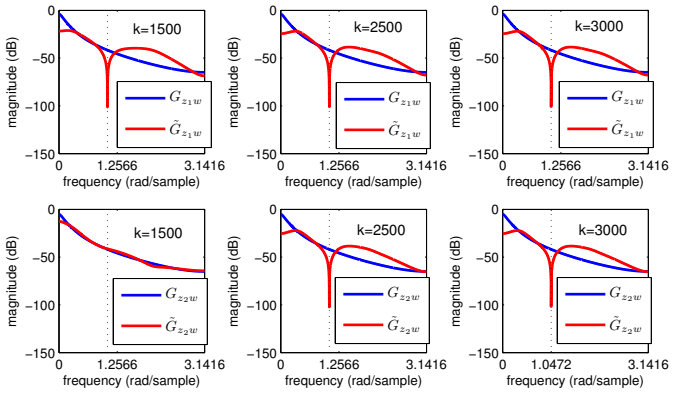

Figure 11. OPEN-LOOP AND CLOSED-LOOP BODE MAGNITUDE PLOTS IN EX. 5.3 AT TIME STEPS $k = 1500, 2500$ AND 3000. BLUE REPRESENTS OPEN-LOOP, RED REPRESENTS CLOSED-LOOP. THE FIRST ROW SHOWS G_{z_1w}, WHEREAS THE SECOND ROW SHOWS G_{z_2w}. COMPARED TO THE OPEN-LOOP LEVELS, ABOUT 60 dB MORE SUPPRESSION IS OBTAINED AT THE COMMAND FREQUENCY 1.0472 RAD/SAMPLE IN BOTH CHANNELS AT $k = 3000$.

these parameters, every eigenvalue of $\bar{A}$ lies in the open left-half plane, and thus the structure is asymptotically stable.

Consider two RCAC controllers $G_{c,1}$, $G_{c,2}$ connected to the structure as in Figure 1. The controller $G_{c,1}$ applies a force $f_1(kh)$ on m_1, and the controller $G_{c,2}$ applies a force $f_4(kh)$ on m_4, and thus, $u_1(k) = f_1(kh)$, $u_2(k) = f_4(kh)$. The controllers have separate performance objectives; $z_1(k) = q_2(kh)$, whereas $z_2(k) = q_3(kh)$, and the disturbance forces $\bar{w}_2(t)$ and $\bar{w}_3(t)$ perturb the structure. The goal of each decentralized controller

is to reject the disturbance forces from the corresponding performance variable. As shown in Figure 12, both channels are nonminimum-phase; $G_{z_1u_1}(z)$ has a NMP sampling zero near -2.3, whereas $G_{z_2u_2}(z)$ has a NMP sampling zero near -2.2. Furthermore, the first Markov parameter corresponding to $G_{z_1u_1}$ is $H_{1,1} = 0.0035$, and the first Markov parameter corresponding to $G_{z_2u_2}$ is $H_{1,2} = 0.0034$. Using the frequency response information of the sampled-data channels, we apply the linear fitting method [19] to bound the phase mismatch for each channel from above by 60 deg. This gives

$$G_{c,1}(\mathbf{q}) = -0.005886\mathbf{q}^{-1} + 0.006596\mathbf{q}^{-2}, \qquad (39)$$

$$G_{c,2}(\mathbf{q}) = -0.005438\mathbf{q}^{-1} + 0.006233\mathbf{q}^{-2}. \qquad (40)$$

Note that since the linear method is used to obtain (39), (40), there is no need to normalize the leading coefficients.

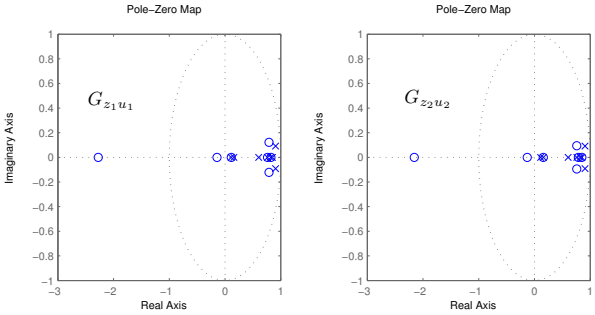

Figure 12. POLES AND ZEROS OF $G_{z_1u_1}(z)$ AND $G_{z_2u_2}(z)$.

We consider the sinusoidal disturbance forces $\bar{w}_2(t) = 100\sin\omega_1 t$ N and $\bar{w}_3(t) = 80\sin\omega_2 t$, where $\omega_1 = 4.488$ Hz and $\omega_2 = 2.856$ Hz. Hence, we have $w(k)\begin{bmatrix} w_1(k) & w_2(k)\end{bmatrix}$, where $w_1(k) = 100\sin\Omega_1 k$, $w_2(k) = 80\sin\Omega_2 k$, $\Omega_1 = 0.8976$ rad/sample, and $\Omega_2 = 0.5712$ rad/sample. The controllers interact with the structure as follows. First, for 500 time steps, the duct is allowed to run open-loop. Next, at $k = 500$, $G_{c,1}$ is turned on for minimizing the displacement $q_2(kh)$. At $k = 3000$, the parameters θ_1 of $G_{c,1}$ are frozen, and $G_{c,2}$ is turned on for minimizing the displacement $q_3(kh)$. Finally, at $k = 6000$, $G_{c,1}$ is allowed to adapt again, so that both controllers adapt simultaneously. The time intervals for individual controller adaptation are chosen to be larger than the previous Examples 5.2 and 5.3, because, typically, it takes longer for RCAC to converge when the plant is nonminimum-phase. The tuning parameters are chosen to be $n_c = 15$ and $P_0 = 0.1I$ for both controllers. Furthermore, since both channels have unknown NMP zeros, we let $\eta_0 = 0.1$, $p_c = 10$ for $G_{c,1}$; $\eta_0 = 0.2$, $p_c = 10$ for $G_{c,2}$. The closed-loop response is illustrated in Figure 13. The closed-loop suppression levels at $k = 3000$, $k = 6000$ and $k = 10000$ are compared with the open-loop level in Figure 14. ■

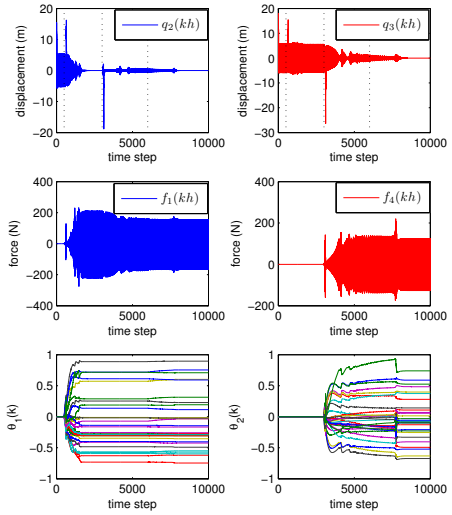

Figure 13. EX. 5.4: TWO DECENTRALIZED RCAC CONTROLLERS TO MINIMIZE $q_2(kh)$, $q_3(kh)$ IN THE PRESENCE OF NMP SAMPLING ZEROS. AT $k = 500$, $G_{c,1}$ IS ACTIVATED AND DRIVES THE PERFORMANCE DISPLACEMENT $q_2(kh)$ TO ZERO. NEXT, AT $k = 3000$, THE PARAMETERS OF $G_{c,1}$ ARE FROZEN, $G_{c,2}$ IS ACTIVATED AND DRIVES $q_3(kh)$ TO ZERO. THE PERFORMANCE $q_2(kh)$ DEGRADES DUE TO THE ACTIVATION OF $G_{c,2}$. HOWEVER, AT $k = 6000$, $G_{c,1}$ IS ALLOWED TO ADAPT AGAIN AND DRIVES $q_2(kh)$ BACK TO ZERO.

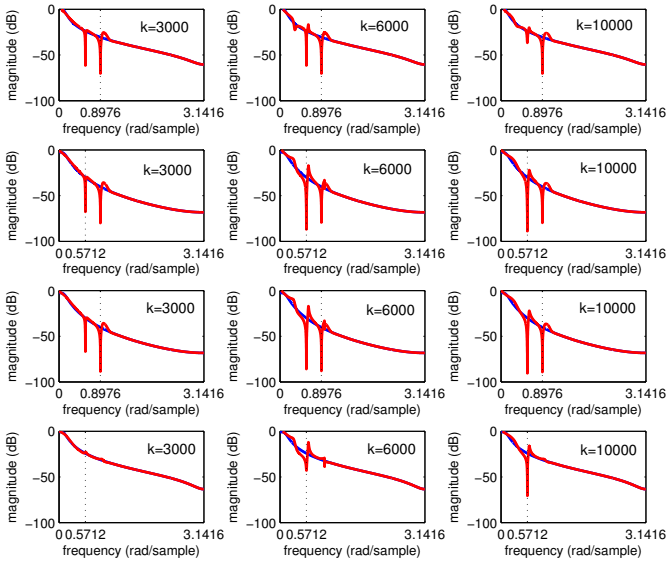

Figure 14. OPEN-LOOP AND CLOSED-LOOP BODE MAGNITUDE PLOTS IN EX. 5.4 AT TIME STEPS $k = 3000$, 6000 AND 10000. BLUE REPRESENTS OPEN-LOOP, RED REPRESENTS CLOSED-LOOP. FIRST ROW SHOWS $G_{z_1w_1}$, SECOND ROW SHOWS $G_{z_1w_2}$, THIRD ROW SHOWS $G_{z_2w_1}$, AND FOURTH ROW SHOWS $G_{z_2w_2}$. DISTURBANCE FREQUENCY IS ATTENUATED AT EACH CHANNEL.

6 CONCLUSION

In this paper, we investigated the stability and performance of retrospective cost adaptive control in a decentralized setting.

We applied adaptive control to investigate the ability of the local controllers to cooperate globally despite uncertainty, lack of communication, and possibly conflicting performance objectives. The application for this study was noise rejection, where it is desirable to implement an active noise control system with independent local controllers that lack the ability to communicate with the other local controllers. When the decentralized controllers share the same performance measure, stability was maintained by scaling the leading coefficient of the filter that is used in retrospective cost optimization. When the decentralized controllers have conflicting performance objectives, noise attenuation was obtained by properly scheduling the adaptation periods of the decentralized controllers.

REFERENCES

[1] Siljak, D. D., 1991. *Decentralized Control of Complex Systems*. Academic Press.

[2] Wang, S. H., and Davison, E., 1973. "On the Stabilization of Decentralized Control Systems". *IEEE Trans. Autom. Contr.,* **18**(5), pp. 473–478.

[3] Jr., N. S., Varaiya, P., Athans, M., and Safonov, M., 1978. "Survey of Decentralized Control Methods for Large Scale Systems". *IEEE Trans. Autom. Contr.,* **23**(2), pp. 108–128.

[4] Corfmat, J. P., and Morse, A. S., 1976. "Decentralized Control of Linear Multivariable Systems". *Automatica,* **12**(5), pp. 479–495.

[5] Witsenhausen, S., 1968. "A Counterexample in Stochastic Optimum Control". *SIAM J. Control,* **6**(1), pp. 131–147.

[6] Sahai, A., and Grover, P., 2010. "Demystifying the Witsenhausen Counterexample". *IEEE Contr. Sys.,* **30**(6), pp. 20–24.

[7] Venugopal, R., and Bernstein, D., 2000. "Adaptive Disturbance Rejection Using ARMARKOV System Representation". *IEEE Trans. Contr. Sys. Tech.,* **8**, pp. 257–269.

[8] Santillo, M. A., and Bernstein, D. S., 2010. "Adaptive Control Based on Retrospective Cost Optimization". *J. Guid. Contr. Dyn.,* **33**, pp. 289–304.

[9] Hoagg, J. B., and Bernstein, D. S., 2010. "Cumulative Retrospective Cost Adaptive Control with RLS-Based Optimization". In Proc. Amer. Contr. Conf., pp. 4016–4021.

[10] D'Amato, A. M., Sumer, E. D., Mitchell, K. S., Morozov, A. V., Hoagg, J. B., and Bernstein, D. S., 2011. "Adaptive Output Feedback Control of the NASA GTM Model with Unknown Nonminimum-Phase Zeros". In AIAA Guid. Nav Contr. Conf.

[11] Hoagg, J. B., Santillo, M. A., and Bernstein, D. S., 2008. "Discrete-Time Adaptive Command Following and Disturbance Rejection with Unknown Exogenous Dynamics". *IEEE Trans. Autom. Contr.,* **53**, pp. 912–928.

[12] Hoagg, J. B., and Bernstein, D. S., 2010. "Retrospective Cost Adaptive Control for Nonminimum-Phase Discrete-Time Systems Part 1: The Ideal Controller and Error System; Part 2: The Adaptive Controller and Stability Analaysis". In Proc. Conf. Dec. Contr., pp. 893–904.

[13] D'Amato, A. M., Sumer, E. D., and Bernstein, D. S., 2011. "Frequency-Domain Stability Analysis of Retrospective-Cost Adaptive Control for Systems with Unknown Nonminimum-Phase Zeros". In Proc. Conf. Dec. Contr., pp. 1098–1103.

[14] Ioannou, P., 1986. "Decentralized Adaptive Control of Interconnected Systems". *IEEE Trans. Autom. Contr.,* **31**(4), pp. 291–298.

[15] Jain, S., and Khorrami, F., 1997. "Decentralized Adaptive Control of a Class of Large-Scale Interconnected Nonlinear Systems". *IEEE Trans. Autom. Contr.,* **42**(2), pp. 136–154.

[16] Narendra, K. S., and Oleng, N. O., 2002. "Exact Output Tracking in Decentralized Adaptive Control Systems". *IEEE Trans. Autom. Contr.,* **47**(2), pp. 390–395.

[17] Astrom, K. J., and Wittenmark, B., 1995. *Adaptive Control*. Addison-Wesley.

[18] Goodwin, G. C., and Sin, K. S., 1984. *Adaptive Filtering, Prediction and Control*. Prentice Hall.

[19] Sumer, E. D., Holzel, M. H., D'Amato, A. M., and Bernstein, D. S., 2012. "FIR-Based Phase Matching for Robust Retrospective Cost Adaptive Control". In Amer. Contr. Conf.

[20] Hong, J., Akers, J. C., Venugopal, R., Lee, M. N., Sparks, A. G., Washabaugh, P. D., and Bernstein, D. S., 1996. "Modeling, Identification, and Feedback Control of Noise in an Acoustic Duct". *IEEE Trans. Contr. Sys. Tech.,* **4**, pp. 283–291.